# Theory and Monte Carlo simulation of the ideal gas with shell particles in the canonical, isothermal-isobaric, grand canonical and Gibbs ensembles

Harold W. Hatch,[1, a)] Vincent K. Shen,[1] and David S. Corti[2]
[1)] *Chemical Informatics Research Group, Chemical Sciences Division, National Institute of Standards and Technology, Gaithersburg, Maryland 20899-8380, USA*
[2)] *Davidson School of Chemical Engineering, Purdue University, West Lafayette, IN 47907-2100, USA*

(Dated: 22 August 2024)

Theories of small systems play an important role in the fundamental understanding of finite size effects in statistical mechanics, as well as the validation of molecular simulation results as no computer can simulate fluids in the thermodynamic limit. Previously, a shell particle was included in the isothermal-isobaric ensemble in order to resolve an ambiguity in the resulting partition function. The shell particle removed either redundant volume states or redundant translational degrees of freedom of the system, and yielded quantitative differences from traditional simulations in this ensemble. In this work, we investigate the effect of including a shell particle in the canonical, grand canonical and Gibbs ensembles. For systems comprised of a pure component ideal gas, analytical expressions for various thermodynamic properties are obtained. We also derive the Metropolis Monte Carlo simulation acceptance criteria for these ensembles with shell particles, and the results of the simulations of an ideal gas are in excellent agreement with the theoretical predictions. The system size dependence of various important ensemble averages is also analyzed. (This is an author reprint. See the published version at https://doi.org/10.1063/5.0224305.)

## I. INTRODUCTION

Although many thermodynamic and statistical mechanical theories are applied in the thermodynamic limit of infinite system sizes,[1] the advent of the molecular simulation of fluids by Metropolis *et al.*[2] led to a necessary interest in small systems. In an attempt to calculate bulk properties from a finite system, molecular simulations commonly avoid the introduction of interacting boundaries through the application of periodic boundary conditions (PBCs).[3,4] Nevertheless, PBCs do not eliminate all finite size effects, as molecular simulations must be performed with a limited number of particles. Consequently, system size effects must be carefully considered in many simulations, as they are important in the calculation of critical properties,[5,6] surface tension,[7] phase equilibrium,[8] diffusion coefficients,[9,10] viscosity,[9,11] pressure,[12] activity coefficients[13] and other thermodynamic properties.[14]

As another example, inconsistencies in the application of the isothermal-isobaric ($NpT$) ensemble to small systems were previously noted. In particular, the original formulation of this ensemble,[15] when the volume is treated as a continuous variable, sums over states for which the volume of the system is not uniquely defined. The resulting partition function therefore had units of volume, which was typically then made dimensionless through division by some arbitrary unit of volume.[16] The volume of the system can be uniquely determined, however, through the use of a "shell particle," where at least one particle resides in the differential volume $\mathrm{d}V$ surrounding the volume $V$.[16–19] Consequently, the shell particle automatically eliminates redundant microstates from the $NpT$ partition function, which is now necessarily dimensionless. While inconsequential for a system with a large number of particles, the use of the shell particle nonetheless yields quantitatively different thermodynamic properties for small systems.[17,18,20,21]

In the derivation of the correct formulation of the $NpT$ ensemble, the system of interest with a fixed number of particles was embedded within a much larger thermal and pressure bath.[17,18] When considering volume fluctuations of the system, a boundary identifying the volume states of the system needed to be introduced, which also served to prevent both the particles in the surroundings from entering the system volume and the particles in the system from leaving the selected volume. Since the boundary was only employed to identify a fluctuated volume state of the system, its effects cannot appear in the final result. The shell particle, via its removal of redundant volume states, accomplished this task. By attaching the boundary to a shell particle, a new and distinct microstate of both the system and bath is necessarily generated when the volume of the system is varied, i.e., a change in volume corresponds to a change in the configuration of the system. Without a shell particle, the boundary can be moved without altering the positions of any of the particles, thereby resulting in no variation of the given microstate.

However, when the system is contained within a volume for which PBCs are applied, as during a molecular simulation, the particles within the system only interact with themselves and not with the particles in the bath. The particle configurations of the system and bath are therefore independent, although the bath still maintains its role as a pressure reservoir that limits the allowed vol-

[a)] Electronic mail: harold.hatch@nist.gov

ume fluctuations of the system. Furthermore, even when a shell particle is not present, a change in the volume of the system automatically generates a new microstate of the system, since a subset of the relative distances between particles varies as the volume is altered. Hence, when PBCs are applied, a shell particle is not needed to define the system volume, i.e., the issue of redundant microstates no longer arises.

Nevertheless, the application of PBCs introduces another set of redundant states that arguably should also be removed. These redundant states follow from the trivial uniform translation of the entire system within the triclinic periodic boundaries. While a shell particle is no longer needed to remove redundant volume states, Han and Son[22] showed for the $NpT$ ensemble that a shell particle, nonetheless, removes these translationally redundant microstates from the partition function. (These redundancies are straightforwardly removed upon introduction of a shell particle, although this is not the only way to eliminate them.) Upon their removal, the correct $NpT$ partition function is still obtained. Yet, some ensemble averages for systems with PBCs are still different from those obtained without PBCs and for which redundant volume states were instead eliminated.[21]

In this article, we consider the impact of the removal of translational redundancies on various thermodynamic properties for systems in which PBCs are applied. These redundancies are eliminated with the use of a shell particle, and we investigate the effect of its introduction into other ensembles, besides just the $NpT$ ensemble. Specifically, for systems with PBCs, we include the shell particle in the grand canonical[23,24] and Gibbs[25] ensembles, which to our knowledge has not been considered before.

Many researchers use Monte Carlo (MC) Gibbs ensemble simulations to study phase behavior in bulk and confined fluids.[25–30] The motivation for considering a shell particle in the Gibbs ensemble[25] is similar to that for the $NpT$ ensemble. In MC simulations of bulk fluids in the Gibbs ensemble with volume transfers,[27] PBCs are separately applied to each system in independent real spaces. The volume transfer between these systems therefore occurs virtually, and not by a flexible membrane or piston. The removal of translational redundancies from both systems with PBCs can be accomplished through the introduction of a shell particle into each system. We consider the resulting finite size effects[31] when a shell particle is or is not employed in this ensemble.

In addition to volume transfer, particles may also transfer between the two coupled systems in the Gibbs ensemble.[25] If a shell particle is used in each system, these Gibbs ensemble simulations must avoid transferring the shell particles. Hence, for particle transfers only, the use of a shell particle gives rise to a minimum density in each system. Particle transfers also occur in grand canonical ensemble simulations, and so the use of a shell particle in these simulations would also yield a minimum density. Preventing the density of the system from becoming too low may have important implications for vapor-liquid equilibrium calculations from flat-histogram simulations in the grand canonical ensemble when the density of the vapor is low.[32] Moreover, when volume transfers also occur in Gibbs ensemble simulations, shell particles with excluded volume should also prevent the volume of either system from approaching a zero size. The introduction of shell particles into the Gibbs ensemble may therefore eliminate a known stability issue that potentially occurs when they are not employed, particularly when there is a large enough probability that one of the systems has no particles and infinitesimal volume during a simulation.[25]

In what follows, we only consider systems composed of a pure component ideal gas in order to demonstrate the impact of the shell particle on various thermodynamic properties. For an ideal gas, theoretical derivations are analytically tractable and yield closed-form expressions for the various probability distributions and ensemble averages of the fluctuating thermodynamic variables. Hence, the differences in these quantities both with and without a shell particle can be determined as the system size increases. In addition, simulations of an ideal gas using Metropolis MC are very straightforward. Because an ideal gas does not interact with itself or the boundaries of the system, the location of any particle need not be explicitly stated; only the total number of particles and the number of shell particles in the ensemble needs to be specified during a simulation. All simulations can therefore be implemented in a few dozen lines of Python code, as included in the Supplemental Online Material, and yield results with relatively small error bars in less than an hour on a single processor. Thus, precise comparisons between the theoretically derived thermodynamic properties and the averages obtained directly from Metropolis MC simulations can be obtained.

This paper is organized as follows. In Section II, we begin with the simplest case of the canonical ensemble, both with and without a shell particle. We then revisit in Section III the previously considered isothermal-isobaric ensemble and discuss the Metropolis MC simulations of an ideal gas. By analogy, we then move to the case of the Gibbs ensemble with only volume transfer in Section IV, considering the standard presentation of no shell particles and the new analysis with a shell particle in each coupled system. The case of particle transfers are first considered in the grand canonical ensemble in Section V and then the Gibbs ensemble with only particle transfers in Section VI. In Section VII, all of these concepts are combined in the Gibbs ensemble with both volume and particle transfers. Finally, conclusions and possible future work are discussed in Section VIII.

## II. CANONICAL ($NVT$) ENSEMBLE

A system in the $NVT$ ensemble has a constant number of particles, $N$, a constant volume $V$ and is maintained at a fixed temperature, $T$. Since the canonical ensemble partition function is utilized in both the Gibbs and

grand canonical ensembles, we briefly consider how the microstates available to the system in the $NVT$ ensemble change when a shell particle is used.

### A. Canonical ensemble without a shell particle

The $NVT$ ensemble partition function for $N$ indistinguishable particles is given by

$$Q = \frac{1}{\Lambda^{dN} N!} \int \mathrm{d}\boldsymbol{r}^N e^{-\beta U}, \tag{1}$$

where $d$ is the number of dimensions, $\Lambda$ is the de Broglie wavelength of a particle, $U$ is the total potential energy of the $N$-particle system, $\beta = 1/(k_B T)$, $k_B$ is the Boltzmann constant and $\mathrm{d}\boldsymbol{r}^N$ are the differential volume elements of all $N$ particles. In the case of an ideal gas, for which $U = 0$, the above reduces to[1]

$$Q = \frac{V^N}{\Lambda^{dN} N!}. \tag{2}$$

All thermodynamic properties can be derived from the partition function. For example, the internal pressure, $p_{int}$, is given by

$$\beta p_{int} = \left.\frac{\partial \ln Q}{\partial V}\right|_{\beta,N} = \frac{N}{V}, \tag{3}$$

which is the familiar ideal gas equation of state.

### B. Canonical ensemble with a shell particle

Consider now the use of a shell particle in the $NVT$ ensemble in order to remove translational redundant microstates when PBCs are applied. With particle 1 being chosen as a reference particle, and with it being held fixed in the differential volume element $\mathrm{d}\boldsymbol{r_1}$, the $NVT$ ensemble partition function for this situation is given by

$$Q^* \, \mathrm{d}\boldsymbol{r_1} = \frac{\mathrm{d}\boldsymbol{r_1}}{\Lambda^{dN}(N-1)!} \int \mathrm{d}\boldsymbol{r}^{N-1} e^{-\beta U}, \tag{4}$$

where $U$ is again the total potential energy of all $N$ particles. With particle 1 held fixed in a given location, it is now distinguishable from the remaining $N-1$ particles. In addition, $Q^* \, \mathrm{d}\boldsymbol{r_1}$ is dimensionless, as it again represents a (weighted) number of microstates.

For a system with PBCs, the chosen fixed location of particle 1 is arbitrary, and the same states contained within $Q^* \, \mathrm{d}\boldsymbol{r_1}$ will be generated by placing particle 1 anywhere within $V$. In other words,[22]

$$Q^* = \frac{N}{V} Q. \tag{5}$$

Starting from the partition function without a shell particle, there are $N$ choices for the reference or shell particle, which generates identical states when located anywhere within $V$.

For the case of an ideal gas, Eq. 5 becomes

$$Q^* = \frac{V^{N-1}}{\Lambda^{dN}(N-1)!}, \tag{6}$$

where the superscript $*$ refers throughout this article to any partition function or ensemble average that includes a shell particle. Since no shell particle is explicitly used in Eq. 5 and therefore the momenta of all particles contribute to the pressure as discussed in Refs. 20 and 21, the pressure of the ideal gas is still obtained using Eq. 3. Nevertheless, as will be shown in Sections IV and VII, averages of the pressure in other ensembles besides the canonical ensemble will be different when the shell particle is or is not present.

In all subsequent derivations in this work, the ideal gas resides in a cubical volume with PBCs, as is typically done in Metropolis MC simulations. When a shell particle is introduced, only one shell particle is used in each system with PBCs. There is no need to conduct the trivial MC simulation of an ideal gas in the $NVT$ ensemble. Whether a shell particle is used or not, the ratio of the microstate probabilities between any two ideal gas states is always unity. Hence, the Metropolis acceptance criterion for a trial particle displacement is also always equal to unity.

## III. ISOTHERMAL-ISOBARIC ($NpT$) ENSEMBLE

Since the use of the shell particle is potentially relevant for other ensembles, we consider here the thermodynamic properties of the ideal gas in the $NpT$ ensemble both with and without a shell particle. We also present the results of MC-$NpT$ simulations of an ideal gas. Such seemingly straightforward simulations are, nonetheless, shown to be a useful tool for quickly verifying the theoretical derivations and may also be used to test the algorithms appearing in more complex MC software. All MC simulation code is provided in the Supplemental Online Material.

### A. Isothermal-isobaric ensemble without a shell particle

For a pure component system with $N$ ideal gas particles exposed to a bath with constant pressure, $p$, and constant temperature, $T$, the $NpT$ ensemble partition function is[4]

$$\Delta = \int_0^\infty \mathrm{d}V Q e^{-\beta p V} = \int_0^\infty \mathrm{d}V \frac{V^N}{\Lambda^{dN} N!} e^{-\beta p V}. \tag{7}$$

Note that the above is not dimensionless, with units of volume. The second integral is evaluated with the help of the Gamma function,[33]

$$\Gamma(n) = (n-1)! = \int_0^\infty x^{n-1} e^{-x} \, \mathrm{d}x, \tag{8}$$

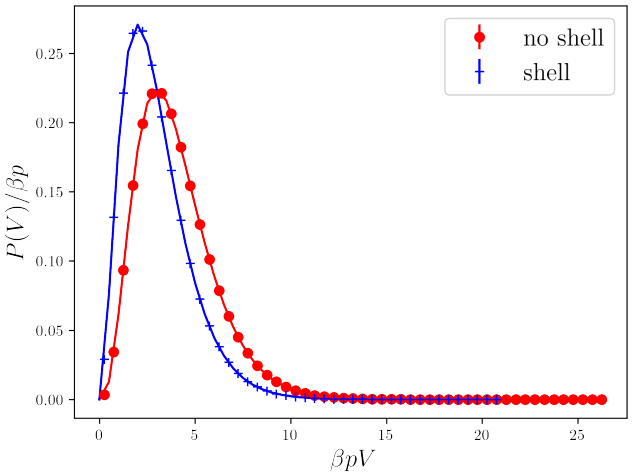


FIG. 1. Probability density of the volume, $V$, nondimensionalized by $\beta p$, of a pure component ideal gas obtained from MC simulations in the isothermal-isobaric ensemble both with (red circles) and without (blue pluses) a shell particle for $N = 3$. Eqs. 10 and 18 are shown by the red and blue lines, respectively. For the MC simulations, the total number of trials was $N_t = 10^7$, volume changes were bounded by $\beta p(\delta V) = 3$ and error bars are standard deviations of the mean and often smaller than the symbols.

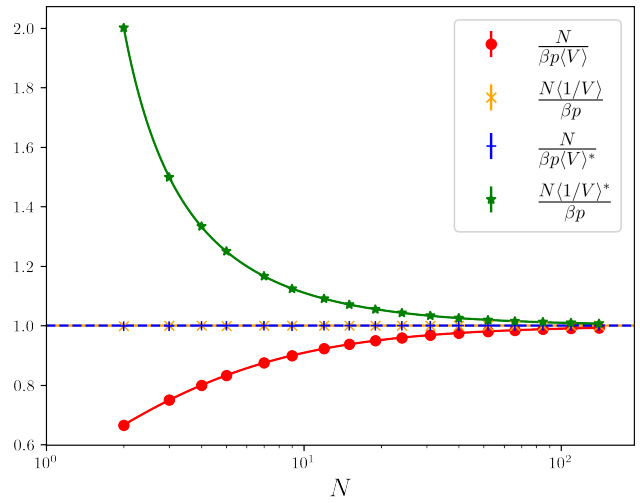


FIG. 2. Various isothermal-isobaric ensemble averages as a function of $N$ for a pure component ideal gas. Ensemble averages with $\langle ...\rangle^*$ include a shell particle, while $\langle ...\rangle$ do not. The four ensemble averages are for each combination of with or without a shell particle, and averages of extensive thermodynamic properties or their inverses. The lines show Eqs. 13, 14, 21 and 22. The symbols are the MC simulation results, with similar details as described in Fig. 1.

where $n$ is a positive integer. Hence, Eq. 7 becomes

$$\Delta = \frac{1}{\Lambda^{dN}} \frac{1}{(\beta p)^{N+1}}. \tag{9}$$

The probability density of finding the system with a given volume is therefore equal to

$$P(V) = \frac{Q}{\Delta} e^{-\beta pV} = (\beta p)^{N+1} \frac{V^N}{N!} e^{-\beta pV}, \tag{10}$$

which is plotted in Fig. 1 for $N = 3$.

Using the above probability density, the ensemble average volume is given by

$$\langle V\rangle = \int_0^\infty \mathrm{d}V V P(V) = \frac{N+1}{\beta p}, \tag{11}$$

where we have again made use of Eq. 8. Because redundancies are included in $\Delta$, this average volume is not exactly the same as $\beta pV = N$. Eq. 11 becomes, however, identical to the equation of state of an ideal gas in the thermodynamic limit.

Next, consider the ensemble average of the inverse volume. Again, using Eq. 10, one finds that

$$\left\langle \frac{1}{V} \right\rangle = \int_0^\infty \mathrm{d}V \frac{1}{V} P(V) = \frac{\beta p}{N}. \tag{12}$$

In finite systems, the ensemble average of the inverse of a fluctuating quantity is not necessarily equal to the inverse of its ensemble average,[34] or $< 1/V > \neq 1/ < V >$. Hence, while Eq. 11 yields

$$\frac{N}{\beta p\langle V\rangle} = \frac{N}{N+1}, \tag{13}$$

the direct ensemble average of the density, obtained using Eq. 12, results in

$$\frac{N\langle 1/V\rangle}{\beta p} = 1. \tag{14}$$

Both averages are plotted vs $N$ in Fig. 2, and become identical as $N$ increases toward the thermodynamic limit. Eq. 14 also indicates, with the use of Eq. 3, that $\langle \beta p_{int}\rangle = \langle \rho\rangle = \beta p$, where $\rho = N/V$.

To further illustrate and test these theoretical derivations, Metropolis MC simulations of an ideal gas were performed in the $NpT$ ensemble without a shell particle. For these simulations, since $U = 0$, there is no need to store the particle positions, and thus no need for particle displacement trial moves. Only the instantaneous volume of the system needs to be sampled. Here, $N_t$ trials were attempted to change the volume uniformly by a random amount within the bounds of $[-\delta V, \delta V]$, and were accepted or rejected according to the Metropolis acceptance probability of $\min(1, \chi)$. $\chi$ is derived based on the ratio of the microstate probability densities, given by Eq. 10, of the newly proposed state and the previous old state,[2,4]

$$\chi = \left(\frac{V_n}{V_o}\right)^N e^{-\beta p(V_n - V_o)}, \tag{15}$$

where $V_o$ is the volume of the old microstate and $V_n$ is the volume of the new microstate.

After an initial equilibration of $10^3$ trials, ensemble averages were obtained from $N_t = 10^7$ trials. Error bars are

included in all MC simulation results throughout this article, and are computed as the standard deviation of the mean obtained by the blocking method,[35] using blocks with a size of $10^2$ trials. Standard deviations of the mean values of the probability densities were obtained from ten blocks. Standard deviations of functions of the ensemble averages were obtained using error propagation. The results of the MC simulations were statistically equivalent to the expected theoretical results, as seen in Figs. 1 and 2.

### B. Isothermal-isobaric ensemble with a shell particle

We now consider the thermodynamic properties of a pure component ideal gas in the $NpT$ ensemble with a shell particle. In this case, the $NpT$ ensemble partition function is given by

$$\Delta^* = \int_0^\infty \mathrm{d}V Q^* e^{-\beta p V} = \int_0^\infty \mathrm{d}V \frac{V^{N-1}}{\Lambda^{dN}(N-1)!} e^{-\beta p V}. \tag{16}$$

Hence, with Eq. 8,

$$\Delta^* = \frac{1}{\Lambda^{dN}} \frac{1}{(\beta p)^N}, \tag{17}$$

which is dimensionless. The probability density of the volume is

$$P^*(V) = \frac{Q^*}{\Delta^*} e^{-\beta p V} = (\beta p)^N \frac{V^{N-1}}{(N-1)!} e^{-\beta p V}, \tag{18}$$

and is shown in Fig. 1 for $N = 3$. With the shell particle, smaller volumes are more likely to occur, as compared to how they are sampled without a shell particle.

The ensemble average of the volume is now given by

$$\langle V \rangle^* = \int_0^\infty \mathrm{d}V V P^*(V) = \frac{N}{\beta p}. \tag{19}$$

The ensemble average of the inverse volume is equal to

$$\left\langle \frac{1}{V} \right\rangle^* = \int_0^\infty \mathrm{d}V \frac{1}{V} P^*(V) = \frac{\beta p}{N-1}, \tag{20}$$

where $N > 1$. Eq. 19 indicates that

$$\frac{N}{\beta p \langle V \rangle^*} = 1 \tag{21}$$

while Eq. 20 requires that

$$\frac{N \langle 1/V \rangle^*}{\beta p} = \frac{N}{N-1}. \tag{22}$$

Both results become identical as the system size increases toward the thermodynamic limit, as also shown in Fig. 2. Furthermore, while $\langle \beta p_{int} \rangle^* = \langle \rho \rangle^*$ for the case of the shell particle, we also have that

$$\langle \beta p_{int} \rangle^* - \frac{\langle \rho \rangle^*}{N} = \beta p, \tag{23}$$

matching a finite system size result previously obtained for a cubical box with PBCs.[20]

Metropolis MC simulations of an ideal gas were also performed in the $NpT$ ensemble with a shell particle. The simulations were performed as described in Section III A, except that the microstate probability with a shell particle, Eq. 18, leads to the following acceptance criterion for volume changes

$$\chi = \left( \frac{V_n}{V_o} \right)^{N-1} e^{-\beta p (V_n - V_o)}. \tag{24}$$

Due to the presence of the shell particle, the above has an exponent of $N-1$ for the volume ratio, instead of the exponent of $N$ appearing in Eq. 15. If volume changes were performed isotropically in $\ln V$ instead of $V$, then the coordinate transformation $P(V)\,\mathrm{d}V \approx P(\ln V) V\,\mathrm{d}\ln V$ would lead to an exponent of $N$ with a shell particle and $N+1$ without a shell particle. The results of the MC simulations with a shell particle were statistically equivalent to the expected theoretical results, as shown in Figs. 1 and 2.

Finally, we discuss another possible interpretation for the need of a shell particle in MC simulations with volume changes and in which PBCs are applied. The shell particle serves to locate a particular position where the affine transformation of isotropic volume changes is centered, and for which the scaling of particle coordinates is required to satisfy detailed balance. If the volume were decreased without altering any of the particle coordinates, any particle positions that subsequently landed outside of the simulation box would then be shifted to another location by the PBCs. The reverse trial move to a larger volume state, again without changing the particle coordinates, would not, however, return those shifted particles to their original locations. Hence, with PBCs, volume moves without the scaling of particle coordinates would not obey detailed balance. In principle, isotropic volume changes with PBCs do not require the center of the system to be identified. Yet, in simulations an origin of the chosen coordinate system is specified, and can therefore be used as the center of an affine transformation. If the positions of all the particles are defined with respect to the location of the shell particle, then the shell particle may be located at the origin for convenience. Hence, the position of the shell particle, unlike the remaining $N-1$ particles, is not scaled during a volume change. The acceptance criterion for volume moves is therefore affected by the presence of the shell particle since it only depends on the number of scaled particle coordinates.

## IV. GIBBS ENSEMBLE WITH VOLUME TRANSFER ONLY

In the $NpT$ ensemble, the system is maintained at mechanical equilibrium by being exposed to a bath at constant pressure. In the Gibbs ensemble, two systems

reach mechanical equilibrium with each other through the transfer of volume between them. Particle transfers also occur in the Gibbs ensemble, but are not yet considered in this section. As in the $NpT$ ensemble, the presence or absence of a shell particle quantitatively affects the resulting thermodynamic properties, as shown using both theoretical derivations and MC simulations.

### A. Gibbs ensemble with volume transfer only between two systems and no shell particles

The volumes of the two systems, $V_1$ and $V_2 = V - V_1$, are allowed to fluctuate, but their total volume, $V$ remains constant, $V_1 \in [0, V]$. The number of particles in the first system, $N_1$, is constant, as are the number of particles in the second system, $N_2 = N - N_1$, where $N$ is the total number of particles (i.e., particles are not transferred between the two systems). The partition function of this composite system without any shell particles is

$$Q_{G,N} = \frac{1}{V\Lambda^{dN}} \int_0^V \mathrm{d}V_1 \frac{V_1^{N_1}}{N_1!} \frac{(V - V_1)^{N-N_1}}{(N - N_1)!}, \tag{25}$$

where division by $V$ makes the partition function dimensionless.[4,36] In order to evaluate this integral, we make use of[37]

$$\int_0^u x^v (u - x)^w \, \mathrm{d}x = u^{v+w+1} \frac{v!w!}{(v + w + 1)!}, \tag{26}$$

in which $v, w > -1$. Hence,

$$Q_{G,N} = \frac{1}{\Lambda^{dN}} \frac{V^N}{(N + 1)!}. \tag{27}$$

The probability density that the first system has a volume $V_1$ is given by

$$P(V_1) = \frac{1}{Q_{G,N}} \frac{1}{V\Lambda^{dN}} \frac{V_1^{N_1}}{N_1!} \frac{(V - V_1)^{N-N_1}}{(N - N_1)!}, \tag{28}$$

which upon substitution of Eq. 27 yields

$$P(V_1) = \frac{(N + 1)!}{V^{N+1}} \frac{V_1^{N_1}}{N_1!} \frac{(V - V_1)^{N-N_1}}{(N - N_1)!}. \tag{29}$$

This probability density is shown in Fig. 3 for $N_1 = 2$ and $N_2 = 4$.

The ensemble average of $V_1$ is given by

$$\langle V_1 \rangle = \int_0^V \mathrm{d}V_1 V_1 P(V_1) = V \left( \frac{N_1 + 1}{N + 2} \right), \tag{30}$$

where we have again made use of Eq. 26. Similarly, $\langle V_2 \rangle = V (N_2 + 1)/(N + 2)$. The ensemble average of the inverse of $V_1$ is

$$\left\langle \frac{1}{V_1} \right\rangle = \int_0^V \mathrm{d}V_1 \frac{1}{V_1} P(V_1) = \frac{N + 1}{VN_1}, \tag{31}$$

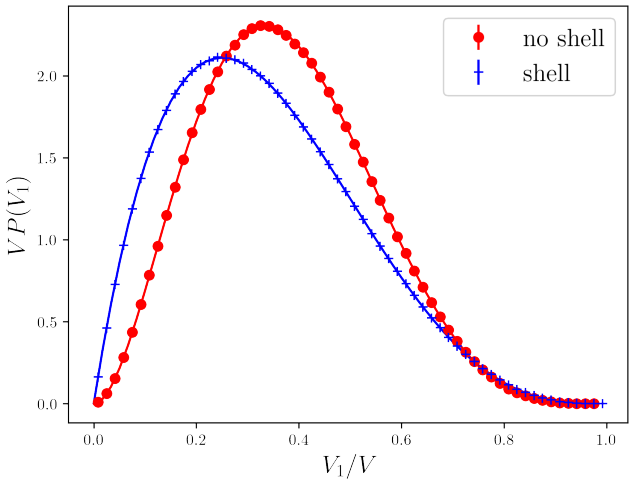


FIG. 3. Probability density of the volume, $V_1$ of the first of two ideal gas systems in the Gibbs ensemble with volume transfers only, nondimensionalized by the total volume, $V$, for $N_1 = 2$ and $N_2 = 4$. The symbols are the MC simulations results for the cases of no shell (red circles) and shell particles in each system (blue pluses), with $N_t = 10^7$ and $\delta V_t = V/3$. The lines show the predictions of Eqs. 29 and 35.

where $N_1 \geq 1$. With a corresponding result for the inverse volume of the second system, along with for example $\beta p_1 = N_1/V_1 = \rho_1$, we have that

$$\langle \beta p_1 \rangle = \langle \rho_1 \rangle = \frac{N + 1}{V} = \langle \rho_2 \rangle = \langle \beta p_2 \rangle . \tag{32}$$

While $\langle \rho_1 \rangle = \langle \rho_2 \rangle$ regardless of the system size (although they are not equal to the bulk density of the entire combined system), $N_1/\langle V_1 \rangle$ and $N_2/\langle V_2 \rangle$ are not equal to each other except in the thermodynamic limit.

Metropolis MC simulations of an ideal gas were also performed in the Gibbs ensemble without a shell particle and with volume transfer only using $N_t$ attempted volume transfer trials between the two systems. These volume transfer trials were performed as follows. The amount of a particular attempted volume transfer was uniformly selected at random between $[0, \delta V_t = 0.5V_1]$. The direction of transfer from system 1 to 2, or 2 to 1, was randomly selected with equal probabilities. The acceptance criterion $\chi$ is again based on the ratio of microstate probabilities of the new proposed state and the old state, which given Eq. 29 results in

$$\chi = \left( \frac{V_{n1}}{V_{o1}} \right)^{N_1} \left( \frac{V_{n2}}{V_{o2}} \right)^{N_2}, \tag{33}$$

where $V_{n1}$ and $V_{o1}$ are the volumes of the first system in the new and old states, respectively, and $V_{n2}$ and $V_{o2}$ are the volumes of the second system in the new and old states, respectively. Error bars were obtained as previously described in Section III. The results of these MC simulations were statistically equivalent to the expected theoretical results, as shown in Figs. 3 and 4.

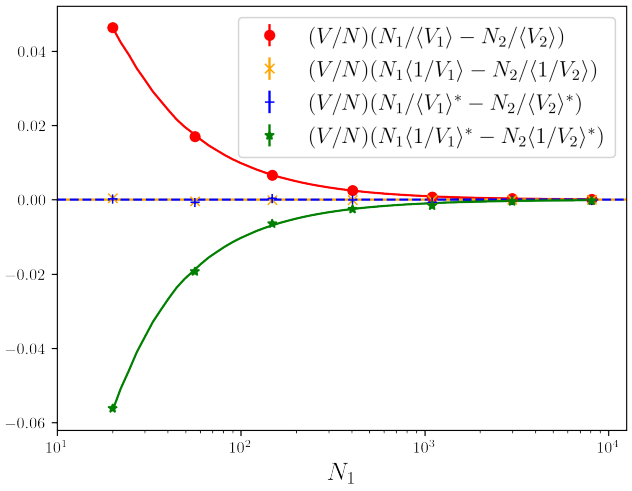


FIG. 4. Various averages in the Gibbs ensemble with volume transfer only as a function of $N_1$ for a pure component ideal gas with $N_1 = 2N_2$ and for which $V/N = 1$. The lines are the predictions of Eqs. 30, 31, 36 and 37, and the symbols show the results of MC simulations with $N_t = 10^6$ and $\delta V_t = V/6$.

### B. Gibbs ensemble with volume transfer only between two systems with shell particles

For the Gibbs ensemble with shell particles and volume transfer only, we explicitly consider the two systems to exist in independent real spaces and both with PBCs. A shell particle is then used in each system to remove the independent set of translational redundancies, as discussed in Section II B. If the two small systems were instead connected by a massless boundary, only one shell particle would be needed to remove the volume redundancies that would now arise. We do not consider this case here.

With a shell particle in each system, the partition function for volume transfers only is now given by

$$\begin{aligned} Q^*_{G,N} &= \frac{V}{\Lambda^{dN}} \int_0^V \mathrm{d}V_1 \frac{V_1^{N_1-1}(V-V_1)^{N-N_1-1}}{(N_1-1)!(N-N_1-1)!} \\ &= \frac{1}{\Lambda^{dN}} \frac{V^N}{(N-1)!}, \end{aligned} \tag{34}$$

where $N_1, N_2 \geq 1$, the multiplication by $V$ ensures $Q^*_{G,N}$ is dimensionless, and we have again made use of Eq. 26. Hence, the probability density that the first system has a volume $V_1$ is

$$\begin{aligned} P^*(V_1) &= \frac{1}{Q^*_{G,N}} \frac{V}{\Lambda^{dN}} \frac{V_1^{N_1-1}}{(N_1-1)!} \frac{(V-V_1)^{N-N_1-1}}{(N-N_1-1)!} \\ &= \frac{(N-1)!}{V^{N-1}} \frac{V_1^{N_1-1}}{(N_1-1)!} \frac{(V-V_1)^{N-N_1-1}}{(N-N_1-1)!}, \end{aligned} \tag{35}$$

which is plotted in Fig. 3 for $N_1 = 2$, $N_2 = 4$ and for which $V/N = 1$. As in Section III, smaller volumes are more likely to be sampled when a shell particle is used as compared to the no shell particle case.

The ensemble average of the volume of the first system is equal to

$$\langle V_1\rangle^* = \int_0^V \mathrm{d}V_1 V_1 P^*(V_1) = V\frac{N_1}{N}. \tag{36}$$

Similarly, $\langle V_2\rangle^* = VN_2/N$. The ensemble average of the inverse of $V_1$ is

$$\left\langle \frac{1}{V_1} \right\rangle^* = \int_0^V \mathrm{d}V_1 \frac{1}{V_1} P^*(V_1) = \frac{N-1}{V(N_1-1)}, \tag{37}$$

where $N_1 \geq 2$. Here, $N_1/\langle V_1\rangle^* = N_2/\langle V_2\rangle^* = N/V$ for all system sizes, while $\langle \rho_1\rangle^* \neq \langle \rho_2\rangle^*$ except in the thermodynamic limit. However, with $\beta p_1 = N_1/V_1$, we find that

$$\langle \beta p_1\rangle^* - \frac{\langle \rho_1\rangle^*}{N_1} = \frac{N-1}{V} = \langle \beta p_2\rangle^* - \frac{\langle \rho_2\rangle^*}{N_2}. \tag{38}$$

The above is, nevertheless, consistent with mechanical equilibrium based on the result for systems with PBCs indicated in Eq. 23.

Metropolis MC simulations of an ideal gas were performed in the Gibbs ensemble with two shell particles and with volume transfers only. The simulations were performed as described in Section IV A, but in this case, the ratio of microstate probabilities obtained from Eq. 35 leads to an acceptance criterion of

$$\chi = \left(\frac{V_{n1}}{V_{o1}}\right)^{N_1-1} \left(\frac{V_{n2}}{V_{o2}}\right)^{N_2-1}. \tag{39}$$

The MC simulation results were again found to be statistically equivalent to the expected theoretical results, as shown in Figs. 3 and 4.

## V. GRAND CANONICAL ($\mu VT$) ENSEMBLE

In the Sections III and IV, we considered mechanical equilibrium of a system with an infinite bath (isothermal-isobaric ensemble) and with another system (Gibbs ensemble with volume transfer only). In this section, we investigate the use of a shell particle in the grand canonical ($\mu VT$) ensemble, in which the volume of the system is fixed, but particles are exchanged with a bath that imposes both a fixed temperature and fixed chemical potential $\mu$. We again present the results for a pure component ideal gas both with and without a shell particle and compare the results of MC simulations to these predictions.

### A. Grand canonical ensemble without a shell particle

The partition function in the $\mu VT$ ensemble is given by[1]

$$\Xi = \sum_{N=0}^{\infty} (z\Lambda^d)^N Q, \tag{40}$$

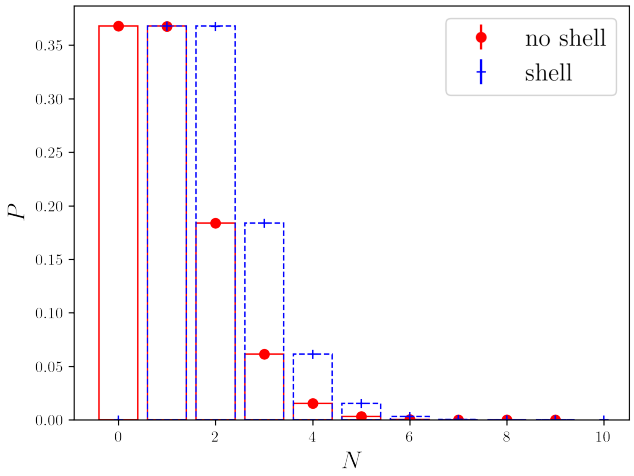


FIG. 5. Probability of the number of ideal gas particles, $N$, in the grand canonical ensemble for $Vz = 1$ both with and without a shell particle. The bars show the predictions of Eqs. 44 (red) and 53 (blue), and the symbols (red circles: no shell; blue plus: shell) are the results of MC simulations with $N_t = 10^7$.

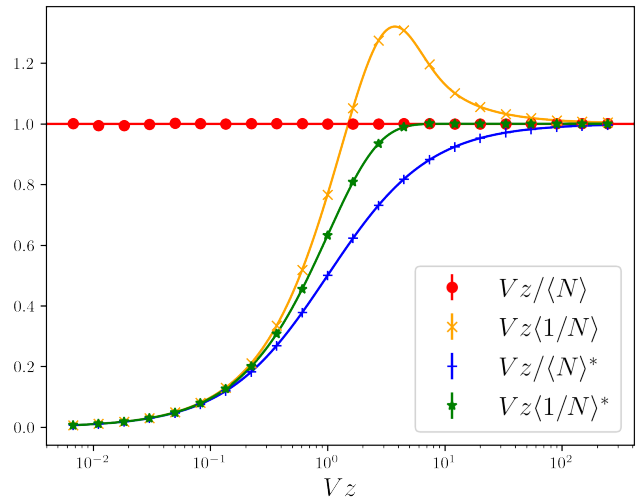


FIG. 6. Various grand canonical ensemble averages as a function of $Vz$ for a pure component ideal gas. The lines show Eqs. 46, 49, 55 and 56 as red, orange, blue and green lines, respectively, while the symbols show the MC simulation results with $N_t = 10^7$ as red circles, orange crosses, blue pluses and green stars, respectively.

where $z = e^{\beta\mu}/\Lambda^d$ is the activity. For a pure component ideal gas, and for which no shell particle is employed, the above becomes after substitution of Eq. 2

$$\Xi = \sum_{N=0}^{\infty} \frac{(Vz)^N}{N!}. \tag{41}$$

Using the following series definition of the exponential function[37]

$$e^x = \sum_{k=0}^{\infty} \frac{x^k}{k!}, \tag{42}$$

Eq. 41 is also equal to

$$\Xi = e^{Vz}. \tag{43}$$

Thus, the probability that the system is found with a given number of particles $N$ is

$$P(N) = \frac{1}{\Xi}\frac{(Vz)^N}{N!} = e^{-Vz}\frac{(Vz)^N}{N!}, \tag{44}$$

which is shown in Fig. 5 for $Vz = 1$.

The ensemble average of $N$ is determined from

$$\langle N\rangle = \sum_{N=0}^{\infty} NP(N) = Vze^{-Vz}\sum_{N=1}^{\infty}\frac{(Vz)^{N-1}}{(N-1)!}, \tag{45}$$

where the $N = 0$ term vanishes. Use of Eq. 42 leads to

$$\langle N\rangle = Vz, \tag{46}$$

which also follows from $\langle N\rangle = z\left(\partial \ln \Xi/\partial z\right)_{\beta,V}$. Hence, $Vz/\langle N\rangle = 1$ for all system sizes, as shown in Fig. 6.

Next, consider the ensemble average of the inverse number of particles. Since $P(N = 0) = e^{-Vz}$ from Eq. 44 is finite and non-zero, the ensemble average of $1/N$ cannot include any microstates for which $N = 0$ because division by zero is an undefined operation. Thus, the ensemble average of this quantity must be calculated as follows:

$$\left\langle \frac{1}{N}\right\rangle = \frac{\sum_{N=1}^{\infty}\frac{1}{N}P(N)}{\sum_{N=1}^{\infty}P(N)} = \frac{e^{-Vz}}{1-e^{-Vz}}\sum_{N=1}^{\infty}\frac{1}{N}\frac{(Vz)^N}{N!}. \tag{47}$$

Using the Puiseux series of the exponential integral, $Ei$,[38]

$$Ei(x) - \ln(x) - \gamma = \sum_{k=1}^{\infty}\frac{x^k}{k(k!)}, \tag{48}$$

where $\gamma$ is the Euler-Mascheroni constant, Eq. 47 can be rewritten as

$$\left\langle \frac{1}{N}\right\rangle = \frac{1}{e^{Vz}-1}[Ei(Vz) - \ln(Vz) - \gamma]. \tag{49}$$

From the limits of $Ei$ for small and large values of its argument, Eq. 49 indicates that $Vz\langle 1/N\rangle \to 0$ as $Vz \to 0$, while $Vz\langle 1/N\rangle \to 1$ as $Vz \to \infty$. These trends are confirmed in Fig. 6, which plots $Vz\langle 1/N\rangle$ vs $Vz$ as obtained from Eq. 49. For a small system ideal gas, $1/\langle N\rangle \neq \langle 1/N\rangle$.

MC simulations of a pure component ideal gas in the $\mu VT$ ensemble were performed without a shell particle as follows. For the ideal gas, the only relevant MC trial move is the insertion or deletion of particles. An insertion or deletion was randomly attempted with equal probabilities. The acceptance criterion follows from the ratio of

microstate probabilities in Eq. 44, resulting in

$$\chi = \frac{N_o!}{N_n!}(Vz)^{N_n - N_o}, \tag{50}$$

where $N_n$ and $N_o$ are the number of particles in the new and old microstates, respectively. For the insertion of a single particle, $\chi = Vz/(N_o + 1)$, and for the deletion of a single particle, $\chi = N_o/(Vz)$.[24] The MC simulation results were statistically equivalent to the expected theoretical results, as seen in Figs. 5 and 6.

### B. Grand canonical ensemble with a shell particle

We now consider the case of a shell particle in the $\mu VT$ ensemble, used again to remove translational redundancies when PBCs are applied. Since the shell particle defines a reference point about which the positions of all other particles are defined, the shell particle cannot be removed from the system; otherwise, the spatial domain of the system would no longer be defined. For this reason, $N \geq 1$, and so the partition function with a shell particle is now given by

$$\Xi^* = \sum_{N=1}^{\infty} (z\Lambda^d)^N Q^* \, \mathrm{d}\boldsymbol{r_1}, \tag{51}$$

where shell particle 1 is held fixed in the differential volume element $\mathrm{d}\boldsymbol{r_1}$. Upon substitution of Eq. 6 into the above, one finds that

$$\Xi^* = \mathrm{d}\boldsymbol{r_1} z \sum_{N=1}^{\infty} \frac{(Vz)^{N-1}}{(N-1)!} = \mathrm{d}\boldsymbol{r_1} z e^{Vz}. \tag{52}$$

The probability of finding the system with a given number of particles, $N \geq 1$, is therefore equal to

$$P^*(N) = \frac{1}{\Xi^*} \frac{\mathrm{d}\boldsymbol{r_1} z^N V^{N-1}}{(N-1)!} = e^{-Vz} \frac{(Vz)^{N-1}}{(N-1)!}. \tag{53}$$

$P^*(N)$ with a shell particle is equivalent to $P(N-1)$ without a shell particle, Eq. 44. This is also shown in Fig. 5, in which the shell particle histogram is simply shifted to the right, by one particle, of the no shell histogram.

The ensemble average of $N$ is given by

$$\langle N \rangle^* = \sum_{N=1}^{\infty} N P^*(N) = e^{-Vz} \sum_{N=1}^{\infty} N \frac{(Vz)^{N-1}}{(N-1)!}. \tag{54}$$

Upon rewriting the second sum and making use of Eq. 42, one finds that

$$\begin{aligned} \langle N \rangle^* &= e^{-Vz} \sum_{N=1}^{\infty} (N-1) \frac{(Vz)^{N-1}}{(N-1)!} + e^{-Vz} \sum_{N=1}^{\infty} \frac{(Vz)^{N-1}}{(N-1)!} \\ &= Vz + 1, \end{aligned} \tag{55}$$

which also follows from $\langle N \rangle^* = z \left( \partial \ln \Xi^* / \partial z \right)_{\beta, V}$. Clearly, $\langle N \rangle^* \to 1$ as $Vz \to 0$.

Since $N \geq 1$, there is a lower bound of $1/V$ for the grand canonical ensemble-averaged density. When there is no shell particle, and for which the $N = 0$ state is allowed, the average density may reach a zero value. While this minimum density may never be reached for large enough systems, it may still be important for and give rise to quantifiable effects in small systems.

The ensemble average of the inverse number of particles with a shell particle is more straightforward to obtain than in Section V A because of the condition of $N \geq 1$. Here,

$$\begin{aligned} \left\langle \frac{1}{N} \right\rangle^* &= \sum_{N=1}^{\infty} \frac{1}{N} P^*(N) = \frac{e^{-Vz}}{Vz} \sum_{N=1}^{\infty} \frac{(Vz)^N}{N!} \\ &= \frac{1 - e^{-Vz}}{Vz}, \end{aligned} \tag{56}$$

again making use of Eq. 42. As $Vz \to 0$, $\langle 1/N \rangle^* \to 1$, as expected. We also have that

$$\langle N \rangle^* \left\langle \frac{1}{N} \right\rangle^* = \frac{\left(1 - e^{-Vz}\right)(1 + Vz)}{Vz}, \tag{57}$$

which goes to 1 as both $Vz \to 0$ and $Vz \to \infty$, but has a maximum around $Vz \approx 1.79$, at which it also has a value of $\approx 1.8$.

Metropolis MC simulations of an ideal gas were also performed in the $\mu VT$ ensemble with a shell particle. The shell particle cannot be among those particles chosen for deletion ($N \geq 1$). The acceptance criterion for insertion and deletion trial moves, as obtained from the ratio of microstate probabilities in Eq. 53, is now

$$\chi = \frac{(N_o - 1)!}{(N_n - 1)!}(Vz)^{N_n - N_o}, \tag{58}$$

where $\chi = Vz/N_o$ for the insertion of a single particle, and $\chi = (N_o - 1)/Vz$ for the deletion of a single particle. Except for this different acceptance criterion, the MC simulations were performed otherwise identically to those described in Section V A. The results of these MC simulations were again statistically equivalent to the expected theoretical results, as shown in Figs. 5 and 6.

## VI. GIBBS ENSEMBLE WITH PARTICLE TRANSFER ONLY

In the grand canonical ensemble, the chemical potential of the system is maintained through chemical equilibrium with a bath of infinite size. In the Gibbs ensemble, two systems reach chemical equilibrium with each other via the transfer of particles between them. Here, we consider particle transfers only between the two systems, each with fixed volumes. Again, as seen in Sections II to VI, the presence or absence of a shell particle quantitatively affects the resulting thermodynamic properties.

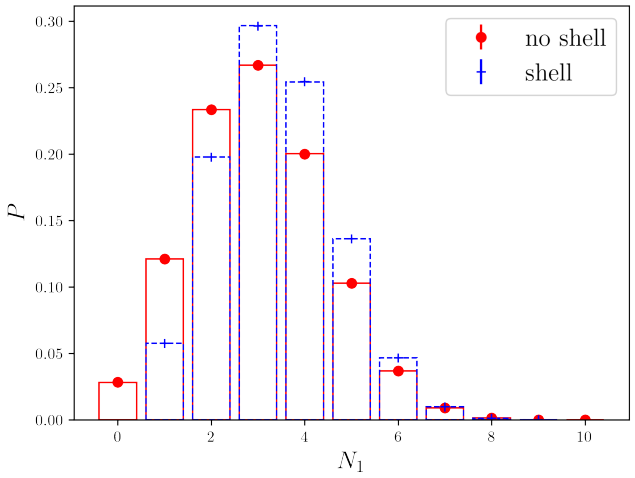


FIG. 7. Probability of the number of ideal gas particles, $N_1$, in the first of two systems within the Gibbs ensemble with particle transfer only. The bars show Eqs. 61 (no shell) and 72 (shell) for $V_1/V = 3/10$ and $N = 10$, while the symbols (red circle, no shell; blue +, shell) show the results of MC simulations with $N_t = 10^7$.

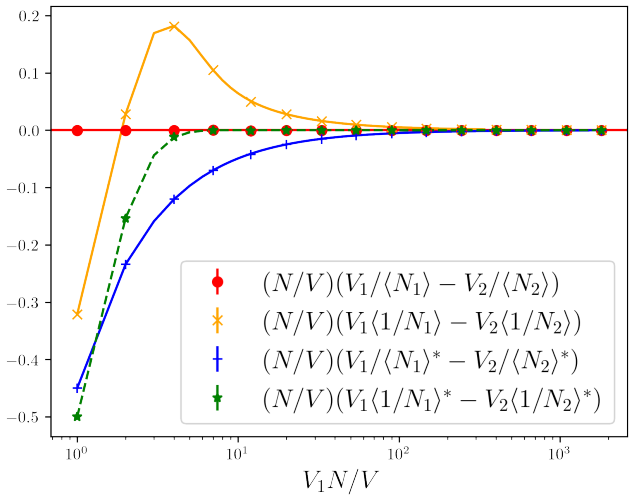


FIG. 8. Various Gibbs ensemble averages with particle transfer only as a function of $V_1N/V$ for a pure component ideal gas, in which $V/N = 1$ and $V_1 = V_2/2$. The lines are Eqs. 66, 67, 76 and 78, and the symbols are the results of MC simulations with $N_t = 10^7$.

### A. Gibbs ensemble with particle transfer only between two systems without shell particles

The number of particles in the two systems, $N_1$ and $N_2 = N - N_1$, is allowed to fluctuate, but the total number of particles, $N$, remains constant, $N_1 \in [0, N]$. The volume of both systems, $V_1$ and $V_2 = V - V_1$, is fixed, as well as the total volume, $V$. The partition function of this ideal gas composite system without any shell particles is

$$Q_{G,V} = \sum_{N_1=0}^{N} \frac{1}{\Lambda^{dN}} \frac{V_1^{N_1}}{N_1!} \frac{(V-V_1)^{N-N_1}}{(N-N_1)!} = \frac{V^N}{N!\Lambda^{dN}}, \quad (59)$$

which was evaluated using the Binomial theorem,[37]

$$(x+y)^n = \sum_{k=0}^{n} \binom{n}{k} x^{n-k} y^k, \quad (60)$$

and for which $\binom{n}{k} = n!/[k!(n-k)!]$. The probability that there are $N_1$ particles in the first system is given by

$$\begin{aligned} P(N_1) =& \frac{1}{Q_{G,V}} \frac{1}{N!\Lambda^{dN}} \binom{N}{N_1} V_1^{N_1} (V-V_1)^{N-N_1} \\ =& \binom{N}{N_1} \left(\frac{V_1}{V}\right)^{N_1} \left(1 - \frac{V_1}{V}\right)^{N-N_1}. \end{aligned} \quad (61)$$

$P(N_1)$ is shown in Fig. 7 for $V_1/V = 3/10$ and $N = 10$. As in Section V A, there is a non-zero probability at $N_1 = 0$, in which $P(N_1 = 0) = (1 - V_1/V)^N$.

The ensemble average of $N_1$ is given by

$$\begin{aligned} \langle N_1 \rangle &= \sum_{N_1=0}^{N} N_1 P(N_1) \\ &= \sum_{N_1=1}^{N} N_1 \binom{N}{N_1} \left(\frac{V_1}{V}\right)^{N_1} \left(1 - \frac{V_1}{V}\right)^{N-N_1}. \end{aligned} \quad (62)$$

To assist in evaluating the above summation, consider the following function:[39]

$$F(s) = \sum_{k=1}^{n} \binom{n}{k} (ps)^k (1-p)^{n-k} = [ps + (1-p)]^n - (1-p)^n, \quad (63)$$

where $0 \le p \le 1$ and

$$F(s=1) = \sum_{k=1}^{n} \binom{n}{k} p^k (1-p)^{n-k} = 1 - (1-p)^n. \quad (64)$$

Independent evaluation of the derivatives of both the left- and right-hand sides of Eq. 63 at $s = 1$ results in

$$\left.\frac{\mathrm{d}F}{\mathrm{d}s}\right|_{s=1} = \sum_{k=1}^{n} k \binom{n}{k} p^k (1-p)^{n-k} = np. \quad (65)$$

Comparing Eq. 65 to Eq. 62, with $p = V_1/V$, indicates that

$$\langle N_1 \rangle = N \frac{V_1}{V}, \quad (66)$$

with a similar result for $N_2$.

Since $P(N_1 = 0) = (1 - V_1/V)^N$ is finite and non-zero, the ensemble average of $1/N_1$ cannot include the $N_1 = 0$

state because division by zero is an undefined operation. Using a similar approach as for the $\mu VT$ ensemble without a shell particle in Section V A, this ensemble average must only include states for which $N_1 \geq 1$, all of which must then be normalized by $1 - P(N_1 = 0)$, or

$$\begin{aligned}\left\langle \frac{1}{N_1} \right\rangle =& \frac{\sum_{N_1=1}^{N} \frac{1}{N_1} P(N_1)}{1 - P(N_1 = 0)} \\ =& \frac{\sum_{N_1=1}^{N} \frac{1}{N_1} \binom{N}{N_1} \left(\frac{V_1}{V}\right)^{N_1} \left(1 - \frac{V_1}{V}\right)^{N-N_1}}{1 - (1 - V_1/V)^N}.\end{aligned} \tag{67}$$

A similar result can be obtained for $\langle 1/N_2 \rangle$, both of which appear to require numerical evaluation. While $V_1/\langle N_1 \rangle$ and $V_2/\langle N_2 \rangle$ are always equal to one another, $\langle V_1/N_1 \rangle \neq \langle V_2/N_2 \rangle$, except in the thermodynamic limit. These trends are shown in Fig. 8.

Metropolis MC simulations of an ideal gas were performed in the Gibbs ensemble without shell particles and with particle transfers only. Particle transfers were performed as follows. The direction of particle transfer from system 1 to 2, or from 2 to 1, was randomly selected with equal probabilities. The acceptance criterion, $\chi$, was obtained from the ratio of the microstate probabilities of the newly proposed state and the old state using Eq. 61,

$$\chi = \frac{N_{o1}!(N - N_{o1})!}{N_{n1}!(N - N_{n1})!} \left(\frac{V_1}{V - V_1}\right)^{N_{n1} - N_{o1}}. \tag{68}$$

We only allowed the transfer of a single particle for each attempted trial move. Hence, for a particle transfer from 2 to 1, $N_{n1} = N_{o1} + 1$ and $\chi = (N - N_{o1})V_1/[(N_{o1} + 1)V_2]$, and for a particle transfer from 1 to 2, $N_{n1} = N_{o1} - 1$ and $\chi = N_{o1}V_2/[(N - N_{o1} + 1)V_1]$. Error bars and histograms were obtained as described in the Section III A. The results of these MC simulations were statistically equivalent to the expected theoretical results, as shown in Figs. 7 and 8.

### B. Gibbs ensemble with particle transfer only between two systems with shell particles

We now consider the case for which PBCs are applied separately to both systems in the Gibbs ensemble. Two shell particles are therefore employed, one in each system, and so $N_1, N_2 \geq 1$ or $N_1 \in [1, N - 1]$. The partition function of this composite system with particle transfer only is given by

$$Q^*_{G,V} = \sum_{N_1=1}^{N-1} \frac{\mathrm{d}\boldsymbol{r_1}\, \mathrm{d}\boldsymbol{r_2}}{\Lambda^{dN}} \frac{V_1^{N_1-1}}{(N_1 - 1)!} \frac{(V - V_1)^{N-N_1-1}}{(N - N_1 - 1)!}, \tag{69}$$

where the shell particles are held fixed in the differential volume elements $\mathrm{d}\boldsymbol{r_1}$ and $\mathrm{d}\boldsymbol{r_2}$. This summation may be rearranged as follows:

$$\begin{aligned}Q^*_{G,V} =& \frac{\mathrm{d}\boldsymbol{r_1}\, \mathrm{d}\boldsymbol{r_2} V^{N-1}}{V_1(N-1)!\Lambda^{dN}} \times \\ & \sum_{N_1=1}^{N-1} N_1 \binom{N-1}{N_1} \left(\frac{V_1}{V}\right)^{N_1} \left(1 - \frac{V_1}{V}\right)^{N-N_1-1},\end{aligned} \tag{70}$$

which, upon comparing to Eq. 65 with $n = N - 1$ and $p = V_1/V$, simplifies to

$$Q^*_{G,V} = \frac{\mathrm{d}\boldsymbol{r_1}\, \mathrm{d}\boldsymbol{r_2} V^{N-2}}{(N-2)!\Lambda^{dN}}. \tag{71}$$

The probability that $N_1$ particles are found in system 1 is equal to

$$\begin{aligned}P^*(N_1) =& \frac{1}{Q^*_{G,V}} \frac{\mathrm{d}\boldsymbol{r_1}\, \mathrm{d}\boldsymbol{r_2}}{\Lambda^{dN}} \frac{V_1^{N_1-1}}{(N_1-1)!} \frac{(V - V_1)^{N-N_1-1}}{(N - N_1 - 1)!} \\ =& \frac{N_1}{(N-1)} \binom{N-1}{N_1} \left(\frac{V_1}{V}\right)^{N_1-1} \left(1 - \frac{V_1}{V}\right)^{N-N_1-1}.\end{aligned} \tag{72}$$

Unlike what was seen for the $\mu VT$ ensemble, there is no simple connection between this shell particle result, $P^*(N_1)$, and the no shell result of $P(N_1)$. $P^*(N_1)$ is shown in Fig. 7 for $V_1/V = 3/10$. At the lower limit of $N_1 = 1$, $P^*(N_1 = 1) = (1 - V_1/V)^{(N-1)} \neq 0$.

The ensemble average of $N_1$ is determined from

$$\begin{aligned}\langle N_1 \rangle^* =& \sum_{N_1=1}^{N-1} N_1 P^*(N_1) = \frac{1}{N-1} \frac{V}{V_1} \times \\ & \sum_{N_1=1}^{N-1} N_1^2 \binom{N-1}{N_1} \left(\frac{V_1}{V}\right)^{N_1} \left(1 - \frac{V_1}{V}\right)^{N-N_1-1}.\end{aligned} \tag{73}$$

Now, returning to Eq. 63, we have

$$\frac{\mathrm{d}^2 F}{\mathrm{d}s^2} = \sum_{k=1}^{n} \binom{n}{k} k(k-1) s^{k-2} p^k (1-p)^{n-k}. \tag{74}$$

After evaluation at $s = 1$, one can show

$$\sum_{k=1}^{n} \binom{n}{k} k^2 p^k (1-p)^{n-k} = np + n(n-1)p^2. \tag{75}$$

Comparing Eq. 75 to Eq. 73, we find

$$\langle N_1 \rangle^* = 1 + (N-2)\frac{V_1}{V}. \tag{76}$$

The influence of the shell particle is seen in the above since $1 \leq \langle N_1 \rangle^* \leq N - 1$ for $0 \leq V_1 \leq V$, as well as $N \geq 2$. Similarly, $\langle N_2 \rangle^* = 1 + (N-2)(1 - V_1/V)$. As also discussed in Section V B, the use of the shell particle in a fixed volume system automatically yields a lower bound on the densities of each system.

The ensemble average of the inverse of $N_1$ is given by

$$\left\langle \frac{1}{N_1} \right\rangle^* = \sum_{N_1=1}^{N-1} \frac{1}{N_1} P(N_1) = \frac{1}{N-1} \frac{V}{V_1} \times \sum_{N_1=1}^{N-1} \binom{N-1}{N_1} \left(\frac{V_1}{V}\right)^{N_1} \left(1 - \frac{V_1}{V}\right)^{N-N_1-1}. \quad (77)$$

Making use of Eq. 64, we have that

$$\left\langle \frac{1}{N_1} \right\rangle^* = \frac{1}{N-1} \frac{V}{V_1} \left[1 - \left(1 - \frac{V_1}{V}\right)^{N-1}\right]. \quad (78)$$

The above indicates that $1/(N-1) \leq \langle 1/N_1 \rangle^* \leq 1$, again since $0 \leq V_1 \leq V$ and $N \geq 2$. Hence, while $\langle 1/N_1 \rangle^* = 1/\langle N_1 \rangle^*$ at the two limiting volumes, these two quantities are otherwise not the same. A similar result follows for system 2, after replacing each subscript 1 with a 2. Consequently, $V_1/\langle N_1 \rangle^* \neq V_2/\langle N_2 \rangle^*$, except in the thermodynamic limit. In addition,

$$\left\langle \frac{V_1}{N_1} \right\rangle^* - \left\langle \frac{V_2}{N_2} \right\rangle^* = \frac{V}{(N-1)} \left[\left(\frac{V_1}{V}\right)^{N-1} - \left(\frac{V_2}{V}\right)^{N-1}\right], \quad (79)$$

which is not equal to zero, except in the thermodynamic limit or if $V_1 = V_2$.

Metropolis MC simulations of an ideal gas were performed in the Gibbs ensemble with shell particles and with particle transfers only. The simulations were conducted as described in Section VI A, except that the acceptance criterion is given by the ratio of the microstate probabilities obtained from Eq. 72,

$$\chi = \frac{(N_{o1}-1)!(N-N_{o1}-1)!}{(N_{n1}-1)!(N-N_{n1}-1)!} \left(\frac{V_1}{V-V_1}\right)^{N_{n1}-N_{o1}}. \quad (80)$$

We again considered the transfer of only a single particle for each attempted trial move. Hence, for a particle transfer from 2 to 1, $N_{n1} = N_{o1} + 1$, $\chi = (N - N_{o1} - 1)V_1/[(N_{o1})V_2]$, and for a particle transfer from 1 to 2, $N_{n1} = N_{o1} - 1$ and $\chi = (N_{o1} - 1)V_2/[(N - N_{o1})V_1]$. These MC simulations yielded results that were statistically equivalent to the expected theoretical predictions, as shown in Figs. 7 and 8.

## VII. GIBBS ENSEMBLE WITH VOLUME AND PARTICLE TRANSFER

For our final case of interest, we consider the Gibbs ensemble with both volume and particle transfers. The two coupled systems are therefore in both mechanical and chemical equilibrium with each other.

### A. Gibbs ensemble with both volume and particle transfers between two systems without shell particles

In the Gibbs ensemble with volume and particle transfers, both the number of particles and volume of each of the two systems fluctuate, while the total number of particles, $N_1 + N_2 = N$, and total volume, $V = V_1 + V_2$, both remain constant. Without a shell particle, the partition function of this composite system is

$$\begin{aligned} Q_G =& \frac{1}{V\Lambda^{dN}} \sum_{N_1=0}^{N} \int_0^V \mathrm{d}V_1 \frac{V_1^{N_1}}{N_1!} \frac{(V-V_1)^{N-N_1}}{(N-N_1)!} \\ =& \frac{1}{V\Lambda^{dN}} \sum_{N_1=0}^{N} \frac{V^{N+1}}{(N+1)!} = \frac{V^N}{\Lambda^{dN} N!}, \end{aligned} \quad (81)$$

where there are $N+1$ identical terms in the last summation. The probability that there are $N_1$ particles in the first system, regardless of its volume, is therefore equal to

$$P(N_1) = \frac{1}{Q_G} \frac{1}{\Lambda^{dN}} \frac{V^N}{(N+1)!} = \frac{1}{N+1}, \quad (82)$$

which is uniform or independent of $N_1$. This is also shown in Fig. 9. Switching the order of the summation and integral in Eq. 81, we also have that

$$Q_G = \frac{V^{N-1}}{\Lambda^{dN} N!} \int_0^V \mathrm{d}V_1, \quad (83)$$

which implies that the probability density of the volume of the first system, regardless of the number of particles it contains, is also uniform since

$$P(V_1) = \frac{1}{Q_G} \frac{1}{\Lambda^{dN}} \frac{V^{N-1}}{N!} = \frac{1}{V}. \quad (84)$$

This probability density is shown in Fig. 10.

The ensemble average of $N_1$, regardless of its volume, is

$$\langle N_1 \rangle = \sum_{N_1=0}^{N} N_1 P(N_1) = \frac{1}{N+1} \sum_{N_1=0}^{N} N_1 = \frac{N}{2}, \quad (85)$$

where we have made use of the triangular number series. For an ideal gas, the two systems therefore have on average the same number of particles. The ensemble average of $V_1$, regardless of the number of particles present in the first system, is

$$\langle V_1 \rangle = \int_0^V \mathrm{d}V_1 V_1 P(V_1) = \frac{1}{V} \int_0^V \mathrm{d}V_1 V_1 = \frac{V}{2}. \quad (86)$$

Thus, the two systems also have on average the same volume. Consequently, $\langle V_1 \rangle / \langle N_1 \rangle = V/N = \langle V_2 \rangle / \langle N_2 \rangle$.

For a given $N_1 \neq 0$ in the first system, the ensemble average of its inverse volume is given by Eq. 31. Thus, in this case, $\langle N_1/V_1 \rangle = (N+1)/V$. However, for $N_1 =$

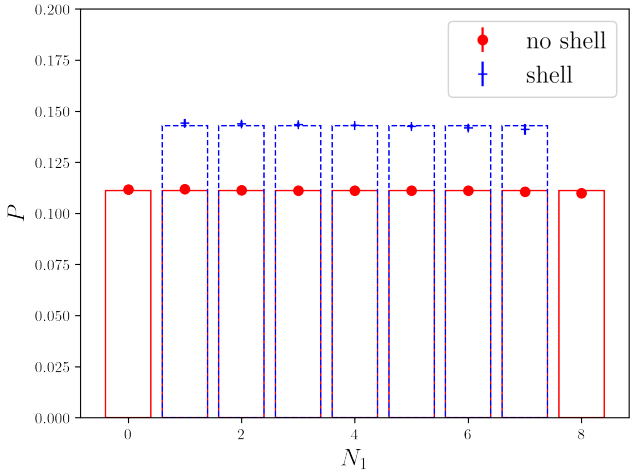


FIG. 9. Probability of the number of ideal gas particles, $N_1$, in the first of two systems, regardless of its volume, in the Gibbs ensemble with both volume and particle transfers for $N = 8$ and $V/N = 1$. The bars show Eqs. 82 and 90, and the symbols indicate the results of MC simulations with $N_t = 10^7$ and $\delta V = 0.05V$.

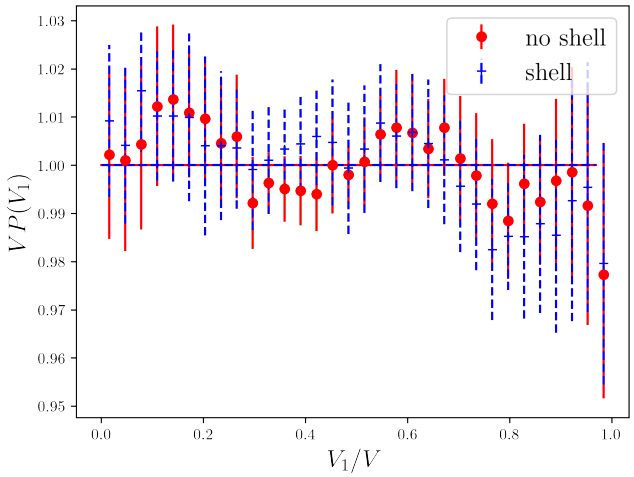


FIG. 10. Probability density of the ideal gas volume, $V_1$, in the first of two systems, regardless of the particle number, in the Gibbs ensemble with both volume and particle transfers for $N = 8$ and $V/N = 1$. The lines show Eqs. 84 and 92, and the symbols indicate the results of MC simulations with $N_t = 10^7$ and $\delta V = 0.05V$.

0, when separately evaluated, $\langle N_1/V_1 \rangle = 0$. Therefore, when averaging over $N_1$, we have that

$$\left\langle \frac{N_1}{V_1} \right\rangle = \sum_{N_1=1}^{N} \frac{N+1}{V} P(N_1) = \frac{N}{V}. \tag{87}$$

Since $\beta p_1 = N_1/V_1$, we also have that $\langle \beta p_1 \rangle = \langle \beta p_2 \rangle$, where $\langle \beta p_2 \rangle = \langle N_2/V_2 \rangle = N/V$.

Since $P(N_1 = 0) = 1/(N+1)$ from Eq. 82 is finite and non-zero, the ensemble average of $\langle V_1/N_1 \rangle$ cannot include

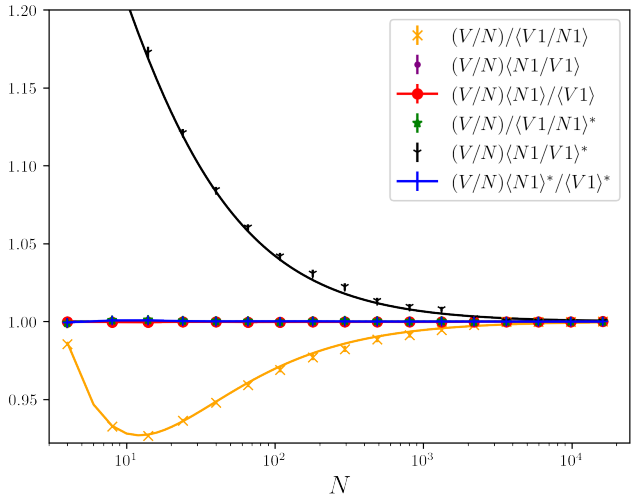


FIG. 11. Various ensemble averages of the density or volume per particle of the first system as a function of $N$, nondimensionalized by $N/V$, for the Gibbs ensemble with both volume and particle transfers. The lines are Eqs. 85, 86, 87, 93, 94 and 95. The symbols show the result of MC simulations as described in Figs. 9 and 10 and with $N_t = 10^7$. Error bars are not included for the ratios of ensemble averages.

any microstates for which $N_1 = 0$ because division by zero is an undefined operation. Using Eq. 30, then

$$\begin{aligned} \left\langle \frac{V_1}{N_1} \right\rangle =& \frac{\sum_{N_1=1}^{N} V \frac{N_1+1}{N_1(N+2)} P(N_1)}{\sum_{N_1=1}^{N} P(N_1)} \\ =& \frac{V}{N+2} \left( 1 + \frac{1}{N} \sum_{N_1=1}^{N} \frac{1}{N_1} \right). \end{aligned} \tag{88}$$

The harmonic series appearing in the last line in the above eventually grows as $\ln N$, so $\langle V_1/N_1 \rangle$ should approach $V/(N+2)$ at large $N$. With a similar result also obtained for the second system, we also have that $\langle V_1/N_1 \rangle = \langle V_2/N_2 \rangle$ regardless of the system size.

Metropolis MC simulations of an ideal gas were performed in the Gibbs ensemble without shell particles using $N_t$ attempted trial moves. For each trial, particle or volume transfers were chosen with equal probability. The acceptance criteria for volume and particle transfers were performed as described in Sections IV A and VI A, respectively. The ratio of microstate probabilities for the volume and particle transfers was performed with fixed $N_1$ or $V_1$, respectively. Because the trials keep one of these variables fixed while changing the other, we did not use the microstate probabilities for $V_1$ at any $N_1$ or for $N_1$ at any $V_1$. Error bars and histograms were obtained as described in Section III A. These MC simulation results were statistically equivalent to the expected theoretical results, as shown in Figs. 9-11.

### B. Gibbs ensemble with both volume and particle transfers between two systems with shell particles

A shell particle is now introduced into each system with PBCs, as discussed in Sections IV B and VI B. Hence, $N_1 \in [1, N-1]$, while both $N$ and $V$ for this composite system are constant. In this case, the partition function is

$$\begin{aligned} Q_G^* =& \frac{V}{\Lambda^{dN}} \sum_{N_1=1}^{N-1} \int_0^V \mathrm{d}V_1 \frac{V_1^{N_1-1}}{(N_1-1)!} \frac{(V-V_1)^{N-N_1-1}}{(N-N_1-1)!} \\ =& \frac{1}{\Lambda^{dN}} \sum_{N_1=1}^{N-1} \frac{V^N}{(N-1)!} = \frac{V^N}{\Lambda^{dN}(N-2)!}, \end{aligned} \tag{89}$$

where there are $N-1$ identical terms in the last summation and we have again made use of Eq. 26. The above also indicates that the probability of the first system having $N_1$ particles, regardless of its volume, is

$$P^*(N_1) = \frac{1}{Q_G^*} \frac{V^N}{\Lambda^{dN}(N-1)!} = \frac{1}{N-1}, \tag{90}$$

which is independent of $N_1$. This is shown in Fig. 9. Switching the order of the summation and integral in Eq. 89, we also have that

$$Q_G^* = \frac{V^{N-1}}{\Lambda^{dN}(N-2)!} \int_0^V \mathrm{d}V_1, \tag{91}$$

which implies that the probability density of the volume of the first system, regardless of its particle number, is also uniform since

$$P^*(V_1) = \frac{1}{Q_G^*} \frac{V^{N-1}}{\Lambda^{dN}(N-2)!} = \frac{1}{V}. \tag{92}$$

The above distribution is the same as the no shell particle case and is also shown in Fig. 10.

The ensemble average of $N_1$ is equal to

$$\langle N_1 \rangle^* = \sum_{N_1=1}^{N-1} N_1 P^*(N_1) = \frac{1}{N-1} \sum_{N_1=1}^{N-1} N_1 = \frac{N}{2}. \tag{93}$$

Since the probability density of the volume is uniform from 0 to $V$, we also have that

$$\langle V_1 \rangle^* = \frac{V}{2}. \tag{94}$$

Both of these averages are the same as for the no shell particle case, and we again find that $\langle V_1 \rangle^* / \langle N_1 \rangle^* = V/N = \langle V_2 \rangle^* / \langle N_2 \rangle^*$. However, unlike the no shell particle case, we found in Section IV B for a fixed value of $N_1$ that $\langle V_1 \rangle^* = N_1 V/N$. Hence, when particle transfers are then allowed, we find that $\langle V_1/N_1 \rangle^* = V/N = \langle V_2/N_2 \rangle^*$. While this equality of the two averages was also obtained for the no shell particle case, the values of these averages are always equal to $V/N$, unlike the no shell particle case.

On the other hand, we may evaluate the ensemble average density of the first system by using Eq. 37, which must exclude $N_1 = 1$ because division by zero is an undefined operation. For $N_1 \geq 2$, the ensemble average of the density of the first system is given by

$$\begin{aligned} \langle \rho_1 \rangle^* =& \frac{\sum_{N_1=2}^{N-1} \frac{N_1(N-1)}{V(N_1-1)} P^*(N_1)}{\sum_{N_1=2}^{N-1} P^*(N_1)} \\ =& \frac{N-1}{V(N-2)} \sum_{N_1=2}^{N-1} \frac{N_1}{(N_1-1)} \\ =& \frac{N-1}{V} \left[ 1 + \frac{1}{N-2} \sum_{N_1=2}^{N-1} \frac{1}{N_1-1} \right], \end{aligned} \tag{95}$$

with a corresponding result for $\langle \rho_2 \rangle^*$. Similar to the no shell particle case, $\langle N_1 \rangle^* / \langle V_1 \rangle^* = \langle N_2 \rangle^* / \langle V_2 \rangle^* = N/V$ for all system sizes and $\langle \rho_1 \rangle^* = \langle \rho_2 \rangle^*$, although the densities do not equal $N/V$ except in the thermodynamic limit. In addition, with $\beta p_1 = N_1/V_1$, we find because of the allowed particle transfer that $\langle \beta p_1 \rangle^* = \langle \beta p_2 \rangle^*$, with $N_1, N_2 \geq 2$.

Metropolis MC simulations of an ideal gas were performed in the Gibbs ensemble with shell particles using volume and particle transfers as described in Sections IV B and VI B, respectively. The MC simulations with a shell particle in the Gibbs ensemble with volume and particle transfers were statistically equivalent to the expected theoretical results, as shown in Figs. 9 and 10. Note when determining ensemble averages of the density, states with only the shell particle present in the system were excluded from the running averages as discussed after Eq. 95.

## VIII. CONCLUSIONS

We have investigated the use of a shell particle in the canonical, isothermal-isobaric, grand canonical, and Gibbs ensembles using both theory and Metropolis MC simulation for an ideal gas. To our knowledge, shell particles have not been previously introduced into any of these ensembles, with the exception of the isothermal-isobaric ensemble. We also considered how various ensemble average properties, both with and without a shell particle, approached their theoretically expected thermodynamic limits. Understanding the system size dependencies of these averages could help in extrapolating the results of Metropolis MC simulations of small systems to the limit of infinite system size, as needed for precise comparison to experimentally measured macroscopic properties.

For systems in which the volume is fixed, such as in the grand canonical ensemble and the Gibbs ensemble with particle transfer only, the use of a shell particle results in a lower bound on the density of the system. This is in contrast with non-shell particle systems where the

zero particle states have a finite probability and may contribute to ensemble averages. Such zero particle states may also have important implications in flat-histogram simulations in the grand canonical ensemble when the density of the vapor is low,[32] which may be the subject of future work.

Ensemble averages presented in this article also exclude those states in which division by zero resulted in an undefined operation. This includes ensemble averages with division by numbers of particles in cases without shell particles in Eqs. 47, 67 and 88, as well as the shell particle case for Gibbs ensemble average density with both volume and particle transfers in Eq. 95. We emphasize that these are averages not typically considered, and we are not aware of any other way to handle such cases.

Moreover, for the complete Gibbs ensemble with both particle and volume transfers, the shell particle may serve to eliminate an instability that can arise for simulations of a non-ideal fluid. In the Gibbs ensemble, when there is a non-zero probability of one of the systems having zero particles, the volume of this zero-particle system may be reduced to infinitesimal amounts due to the absence of particles. With both the volume near zero and containing no particles, the re-insertion of a particle with excluded volume can then prove difficult in a simulation, as the volume first needs to fluctuate to a large enough size in order to accommodate a particle. Such an instability typically arises for Gibbs ensemble simulations near the critical point.[25] The use of shell particles with excluded volume should prevent the sampling of such states in a simulation, thereby improving the estimates of the various phase diagrams obtained with the Gibbs ensemble. This potential benefit of a shell particle requires further study in non-ideal systems.

In this article, we studied the ideal gas because it yielded closed-form expressions that we validated with fast Monte Carlo simulations and systematically compared results with and without shell particles. Despite its simplicity, the ideal gas represents an important starting point for investigating the impact of the shell particle. Unfortunately, the impact of the shell particle on computed properties of non-ideal fluids, such as critical properties, surface tension, and phase equilibrium, cannot be investigated using the ideal gas. Examining other properties and fluids in the current context will be the focus of future work.

## IX. SUPPLEMENTAL ONLINE MATERIAL

The Supplemental Online Material contains the following:

- ideal_gas_mc.ipynb includes all Python code used in this work for the MC simulations and generation of figures.
- ideal_gas_mc.html is a read-only export of ideal_gas_mc.ipynb that may be more convenient to open.
- fig_data.zip contains data for all figures in the comma-separated value format.

## X. DISCLAIMER AND ACKNOWLEDGEMENTS

Contribution of the National Institute of Standards and Technology, not subject to U.S. Copyright. Certain commercial firms and trade names are identified in this document in order to specify the installation and usage procedures adequately. Such identification is not intended to imply recommendation or endorsement by the National Institute of Standards and Technology, nor is it intended to imply that related products are necessarily the best available for the purpose.

[1] T. L. Hill, *An Introduction to Statistical Thermodynamics* (Dover Publications, New York, 1987).
[2] N. Metropolis, A. W. Rosenbluth, M. N. Rosenbluth, A. H. Teller, and E. Teller, J. Chem. Phys. **21**, 1087 (1953).
[3] M. P. Allen and D. J. Tildesley, *Computer simulation of liquids* (Clarendon Press, Oxford, UK, 1989).
[4] D. Frenkel and B. Smit, *Understanding Molecular Simulation: From Algorithms to Applications* (Academic Press, 2002).
[5] A. Z. Panagiotopoulos, Int. J. Thermophys. **15**, 1057 (1994).
[6] A. Z. Panagiotopoulos, J. Chem. Phys. **116**, 3007 (2002).
[7] J. R. Errington, Phys. Rev. E **67**, 012102 (2003).
[8] L. G. MacDowell, V. K. Shen, and J. R. Errington, J. Chem. Phys. **125**, 034705 (2006).
[9] I.-C. Yeh and G. Hummer, J. Phys. Chem. B **108**, 15873 (2004).
[10] O. A. Moultos, Y. Zhang, I. N. Tsimpanogiannis, I. G. Economou, and E. J. Maginn, J. Chem. Phys. **145**, 074109 (2016).
[11] S. H. Jamali, R. Hartkamp, C. Bardas, J. Söhl, T. J. H. Vlugt, and O. A. Moultos, J. Chem. Theory Comput. **14**, 5959 (2018).
[12] G. Hummer, N. Gronbech-Jensen, and M. Neumann, J. Chem. Phys. **109**, 2791 (1998).
[13] J. M. Young and A. Z. Panagiotopoulos, J. Phys. Chem. B **122**, 3330 (2018).
[14] J. C. Palmer, F. Martelli, Y. Liu, R. Car, A. Z. Panagiotopoulos, and P. G. Debenedetti, Nature **510**, 385 (2014).
[15] E. A. Guggenheim, J. Chem. Phys. **7**, 103 (1939).
[16] G. J. M. Koper and H. Reiss, J. Phys. Chem. **100**, 422 (1996).
[17] D. S. Corti and G. Soto-Campos, J. Chem. Phys. **108**, 7959 (1998).
[18] D. S. Corti, Phys. Rev. E **64**, 016128 (2001).
[19] Z. Li and D. S. Corti, Mol. Simul. **44**, 1461 (2018).
[20] D. S. Corti, Mol. Phys. **100**, 1887 (2002).
[21] M. J. Uline and D. S. Corti, Entropy **15**, 3941 (2013).
[22] K.-K. Han and H. S. Son, J. Chem. Phys. **115**, 7793 (2001).
[23] G. E. Norman and V. S. Filinov, High Temp. **7**, 216 (1969).
[24] D. J. Adams, Mol. Phys. **29**, 307 (1975).
[25] A. Z. Panagiotopoulos, Mol. Phys. **61**, 813 (1987).
[26] A. Z. Panagiotopoulos, Mol. Phys. **62**, 701 (1987).
[27] A. Z. Panagiotopoulos, Fluid Ph. Equilib. **76**, 97 (1992).
[28] G. Orkoulas and A. Z. Panagiotopoulos, J. Chem. Phys. **101**, 1452 (1994).
[29] M. G. Martin and J. I. Siepmann, J. Phys. Chem. B **102**, 2569 (1998).
[30] T. R. Josephson, P. J. Dauenhauer, M. Tsapatsis, and J. I. Siepmann, J. Comput. Sci. **48**, 101267 (2021).
[31] J. Recht and A. Panagiotopoulos, Mol. Phys. **80**, 843 (1993).
[32] K. S. Rane and J. R. Errington, J. Phys. Chem. B **117**, 8018 (2013).

[33]E. W. Weisstein, "Gamma Function," (2024), https://mathworld.wolfram.com/GammaFunction.html.
[34]D. S. Corti, D. Ohadi, R. Fariello, and M. J. Uline, J. Phys. Chem. B **127**, 3431 (2023).
[35]H. Flyvbjerg and H. G. Petersen, J. Chem. Phys. **91**, 461 (1989).
[36]B. Smit and D. Frenkel, Mol. Phys. **68**, 951 (1989).
[37]I. S. Gradshteyn and I. M. Ryzhik, *Table of Integrals, Series, and Products* (Academic Press, Inc., New York, USA, 1980).
[38]E. W. Weisstein, "Exponential Integral," (2024), https://mathworld.wolfram.com/ExponentialIntegral.html.
[39]G. Grimmett and D. J. A. Welsh, *Probability: An Introduction* (Oxford University Press, 2014).